특별강연 II

Rheological Analysis in a Spinning Process of a hollow fiber membrane

Moon-Seog Jang

JINRO Central Research Institute

1. Introduction

In the dry-jet-wet-spinning process of a hollow fiber membrane, the polymer solution is pumped into a coaxial tube, jet spinneret. The threadline emerging from the spinneret is stabilized by an internal coagulating medium(liquid or gas) as it emerges from the jet orifice. The nascent hollow thread is further stabilized in a quench bath as shown in Fig. 1. In this scheme, three mechanism of formatiom(temperature gradient, solvent evaporation, and solvent-nonsolvent exchange) can be combined. The changes which promote stabilization often play a dominant role in determining the ultimate fiber wall structure as well. Hence, in pratice, hollow fiber stabilization and development of membrane structure are commonly inseparable.[1] However, fiber dimension(the inside diameter and wall thickness of the hollow fiber) is mainly a rheological problem and is determined by dope pumping rate, spinneret diatance from the coagulation bath, inner coagulant flow rate, and fiber draw-rate.[2] Besides rheological phenomena play a prominent part in the final properties of the hollow fiber.[3]

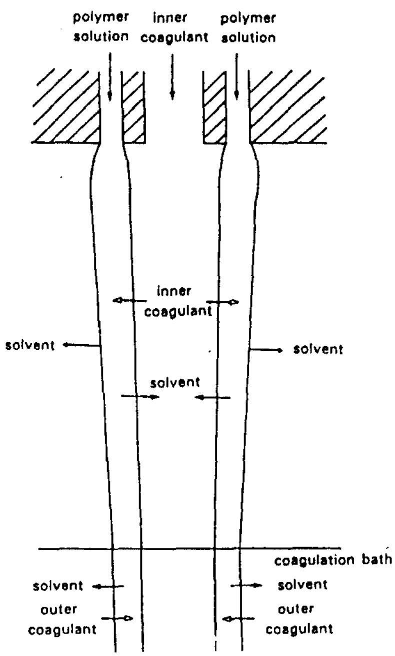

Fig. 1 Flow distribution of hollow fiber spinning.

In the stratified two phase flow problem such as this system, the polymer solution and the inner coagulant flow rate contacted at the interface. This type of flow occurs frequently in engineering applications: in polymer processing(bicomponent fiber, multilayer flat film, coextruded cables and wires).[4] The common characteristic of all these processes is the existence of one or more interface whose position is unknown a priori(free surface problem). And there are additional complexities due to a pressure discontinuity and normal viscous stress jumps. The discontinuity arises due to the finite jump in the fluid properties at the interface, since the interface is modeled as a surface with zero thickness.

The technique allows the finite-element grid itself to be discontinuous at the primitive variables(velocities and pressure) on two different nodes at the same spatial location(double nodes along the interface).[5]

In our work, the spinning process of the hollow fiber from the spinneret tip to the surface of the coagulating bath was simulated by the double-node finite-element method. The calculated dimensions of hollow fibers were compared to the observed dimension of the spun fibers under the same spinning sconditions.

2. Theory

To establish a mathematical model of spinning process of a hollow fiber, the following assumptions were made for the problem:

(1) The flow is in an isothermal steady state.

(2) The polymer solution is an incompressible power-law fluid.

(3) The inner coagulant is an incompressible Newtonian fluid.

(4) Mass transfer between the interface of two phases is negligible.

(5) The effects of surface tension are neglected.

The governing equation include the mass continuity equation and the conservation of momentum:

continuity equation;

$$\nabla \cdot V = 0 \tag{1}$$

momentum equation;

$$\rho V \cdot \nabla V = -\nabla P + \nabla \cdot \underline{\tau} + \rho \tag{2}$$

The symbols V, ρ, P, $\underline{\tau}$ and g refer to velocity vector, the density of fluid, pressure, stress tensor and gravity vector respectively. In addition, the constitutive equation relating the stress tensor to the rate of strain tensor, $\underline{\dot{\gamma}}$, is given as follow.

$$\underline{\dot{\gamma}} = \nabla V + \nabla V^{t} \tag{3}$$

for the Newtonian fluid

$$\underline{\tau} = \mu \underline{\dot{\gamma}} \ (\mu \text{ is constant}) \tag{4}$$

for the power-law fluid

$$\underline{\tau} = \eta \underline{\dot{\gamma}} = m \gamma^{n-1} \underline{\dot{\gamma}} \tag{5}$$

The galerkin finite-element formulation of the above system proceeds by expanding the unknown velocity and pressure fields in a suitable set of basis functions:

$$V = \Sigma V_i \psi_i \tag{6}$$

$$P = \Sigma P_i \varphi_i \tag{7}$$

where V_i, P_i are nodal variables, ψ_i is the quadratic interpolation function for the velocity and φ_i is the linear interpolation function for the pressure. The approximation, Eqs. 6 and 7 are inserted into Eqs. 1 and 2. The resulting momentum residuals are weighted with the velocity basis functions and the continuity residuals with the pressure basis functions. The weighted residuals are intergrated over the solution domain and set to zero, i.e.:

$$R_i^m = \int_\Omega \varphi_i (\nabla \cdot V)\, d\Omega = 0 \tag{8}$$

$$R_i^m = \int_\Omega \psi_i (-\nabla P + \nabla \cdot \tau + \rho g - \rho V \cdot \nabla V) d\Omega = 0 \tag{9}$$

where Ω denotes the small subdomain. The Eq. 9 is intergrated by parts(i.e. applying the divergence theorem) and the constitutive relation is substituted.

$$R_i^m = \int_\Omega \nabla\Psi_i(PU+\eta(\nabla V+\nabla V^t))+\rho\Psi_i(g-V\cdot\nabla V)d\Omega-\int_{\partial\Omega}\Psi_i(n\cdot(-PU+\eta(\nabla V+\nabla V^t)))ds=0 \quad (10)$$

where U is unit tensor, Ω denotes the boundary of the domain, as denotes line intergral along the boundary. Eqs. 8 and 10, when applied at the nodes of the discretized flow domain the appropriate boundary conditions, provide as many as there are unknown nodal velocity and pressure variables.

For free surface problems the free surface location is not known a priori. It is necessary to determain the position of free surface and interface of immiscible fluid. The free surface is a stream surface on which the normal velocity is zero, and the same is applied at the the interface. In the case of interface, the finite element grid is constructed with double nodes. The iterative technique for both cases is successive itreation.

3. Experimental

A polymer solution consisting of 24:40:36 weight percent of cellulose acetate, acetone and formamide was prepared and loaded into the reservoir of one-liter capacity. The solution was extruded through a tube-in-orifice type spinneret by means of nitrogen pressure. Simultaneously a mixture of water and acetone was injected into the inner tube to control the morphological structure of the fiber wall and bore dimensions. The coagulation bath was maintained at a temperature between 2 to 4℃. The fiber so produced was taken up and wound around a pulley type bobbin, and stored wet until it was used for testing. It was found that the wall structure of hollow fibers, spun by injecting an inner coagulant solution of water and aceton in the ratio of 30:70 have shown a fair degree of asymmetricity under a scanning electron mocroscope with relatively dense skin along the outer surface and a microporous layer within.

To photograph the threadline of a nascent hollow fiber during the spinning process, a Nikon stereo photomicroscope of 10 times with an equipped camera was used. And wet fibers frozen in liquid nitrogen was broken and the cross sections of hollow fibers in wet state was photographed by using a Nikon photomicroscope at 40 times.

The viscosity of a polymer solution was measured by using a capillary viscometer.[6] The power-law index of the polymer solution used was found to be 0.6386 and constant, to be 2500.

4. Results and discussion

Flow domain and finite element mesh configurations were shown in Fig. 2. In this numerical simulation, we chose 256 finite elements.

The boundary conditions for this problem were:

(1) at the solid wall of BF, FG, CG, DH;

$v_r = 0,\ v_z = 0$

(2) at the entrance of AB;

$v_r = 0,\ v_z = F_1(r)$

The fuction $F_1(r)$ was obtained from a fully developed pipe flow equation for a Newtonian Fluid with the measured flow rate of the inner coagulant.

(3) at the entrance of CD;

$v_r = 0, \ v_z = F_2(r)$

The fuction $F_2(r)$ was obtained from a fully developed pipe flow equation for a power-law Fluid with the measured flow rate of the polymer solution.

(4) at the centerline of AI;

$v_r = 0, \ \tau_{rz} = 0$

(5) at the surface of a coagulant medium of IJ;

$v_r = 0, \ (\partial v_z / \partial z) = 0$

(6) at the surface of a coagulant medium of JK;

$v_r = 0, \ v_z = v_L$

(7) on the free surface of HK;

$\tau_{nn} = 0, \ \tau_{nt} = 0$

(8) on the interface of GJ;

$V_1 = V_2, \ \tau_1 = \tau_2$

where subscript 1 represent a polymer solution phase and 2, the inner coagulant phase, n is a component tangential to the interface. Calculations were performed for conditions which is the same as the conditions used in the actual spinning process. The under-relaxation scheme was introduced and the convergency was found to be slow(9~12 iterations) for free surface and the interface position.

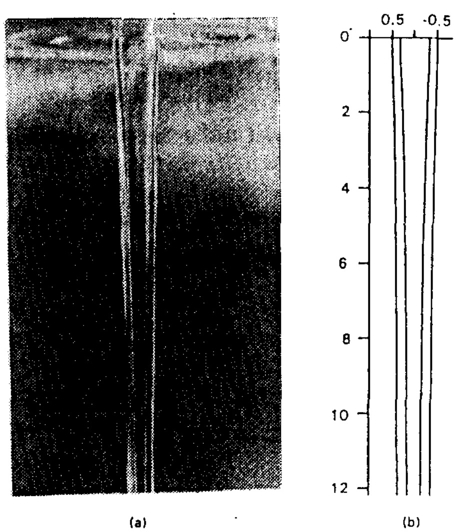

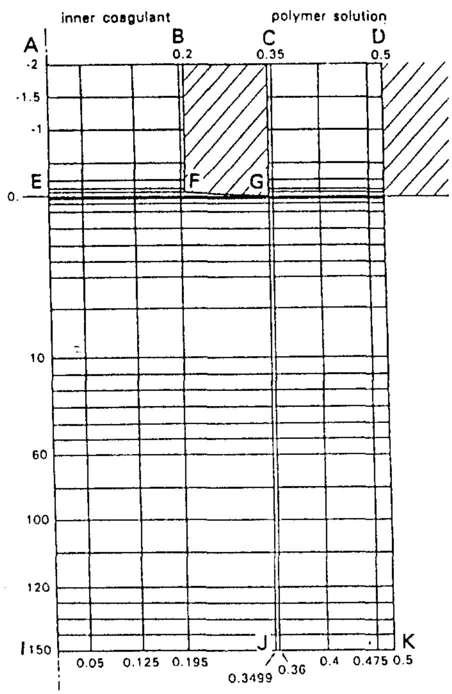

Fig. 2 Finite element grid system

Fig. 3 The threadline of hollow fiber just coming out of the spinneret, dimension in mm.

(a) Photomicrograph of hollow fiber spinning

(b) Simulated threadline of hollow fiber spinning

The photographed threadline of hollow fiber just coming out of the spinneret is shown in Fig. 3 (a) is the photomicrograph of hollow fiber threadline and (b) shows the calculated threadline. The maximum error is 16%. Fig. 4 shows the plots of calculated and observed diameters of the hollow fiber with the lines are the calculated values and the squares are the observed values. The computational results were found to be relatively good agreement with the dimensions of the nascent fiber produced.

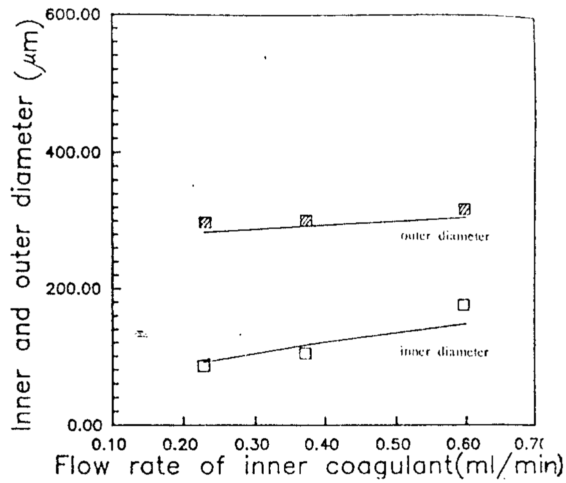

Fig. 4 Diameter of fiber vs. flow rate of inner coagulant, spinning height: 15cm, extrusion rate: 1.92cm^3/min, take-up speed: 56.5m/min, ■ outer diameter, □ inner diameter, — simulated.

5. Conclusions

The spinning process of hollow fiber from the spinneret tip tp the surface of the coagulating bath was simulated sucessfully by the double-node finite-element method. The calculated dimensions of hollow fibers were in good agreement with the observed dimensions of the spun fibers on the same spinning conditions. In summary the spinning variables that control both the fiber dimensions and their morphology were clarified in order to facilitate a further study on hollow fiber production.

Literature cited

(1) I. Cabasso, Hollow Fiber Membranes, Encyclopedia of chemical Technology, 12, 492(1981).

(2) C. D. Han, Multiphase Flow in Polymer processing, Academic Press, New York, 1982.

(3) R. McKinney, Jr., fesalination, 62, 37(1987).

(4) P. Aptel, N. Abidine, F. Ivaldi and J. P. Lafaille, J. of Membrane Science, 22, 199(1985).

(5) H. Mavridis, A. N. Hrymak and J. Vlachopoulos, AIChE J., 33, 410(1987).

(6) J. A. Brydson, Flow Properties of Polymer Melts, 2nd Ed., George Godwin Ltd., 1981

(7) R. B. Bird, R. C. Armstrong and O. Hassager, Dynamics of Polymeric Liquids, Vol. 1, 2nd Ed., 1987